

Supplementary Materials for

Life-threatening influenza and impaired interferon amplification in human IRF7 deficiency

Michael J. Ciancanelli, Sarah X. L. Huang, Priya Luthra, Hannah Garner, Yuval Itan, Stefano Volpi, Fabien G. Lafaille, Céline Trouillet, Mirco Schmolke, Randy A. Albrecht, Elisabeth Israelsson, Hye Kyung Lim, Melina Casadio, Tamar Hermesh, Lazaro Lorenzo, Lawrence W. Leung, Vincent Pedergrana, Bertrand Boisson, Satoshi Okada, Capucine Picard, Benedicte Ringuier, Françoise Troussier, Damien Chaussabel, Laurent Abel, Isabelle Pellier, Luigi D. Notarangelo, Adolfo García-Sastre, Christopher F. Basler, Frédéric Geissmann, Shen-Ying Zhang, Hans-Willem Snoeck, Jean-Laurent Casanova*

*Corresponding author. E-mail: jean-laurent.casanova@rockefeller.edu

Published 26 February 2015 on *Science Express*
DOI: 10.1126/science.aaa1578

This PDF file includes:

Case Report

Materials and Methods

Supplementary Text

Figs. S1 to S9

Tables S1 to S7

References

Supplementary Materials:

Case report

We report the case of a girl born in 2008. According to her medical history, she was born after 39 weeks of gestation with a birth weight of 3910 g and Apgar score 10/10. There was a rash suggestive of measles after the MMR vaccine (at the age of one year). Seven months after this MMR vaccine, she had a new rash with fever evoking measles diagnosed by her pediatrician. Eleven months later she received a new measles, mumps and rubella vaccine without complications. She did not receive vaccination against influenza virus at that time. She had multiple episodes of bronchiolitis, one with hospitalization at the age of 18 months.

In January 2011, she presented with fever and a cough. In less than 24 hours, breathing difficulties progressively appeared and hospitalization in a secondary hospital was ordered. During auscultation, wheezing and crackles were noted in both lung fields accompanied by polypnea. The neurological examination was normal. Laboratory tests performed 72 hours after the onset of the fever showed a moderate leukocytosis with a predominance of neutrophils, moderate hyponatremia (132 mmol/L), and an inflammatory syndrome with C-reactive protein levels at 90 mg/L. The chest radiography showed bilateral diffuse opacities. She was initially treated with an association of ceftriaxone, roxithromycin and vancomycin. A search for viruses and bacteria was carried out on the sputum. Only influenza A/H1N1 was positive with influenza antigen immunoassays (Becton Dickinson Directigen A+B). No secondary or concomitant bacterial infection occurred. Oseltamivir treatment was started at a dose of 45 mg two times a day.

She was quickly transferred from a ward of general pediatrics in a primary care hospital to a pediatric intensive care unit (PICU) in a tertiary university hospital, since increased oxygen was required (her oxygen saturation level was between 88 and 93% and she needed nasal oxygen therapy at more than 5 l/min). She developed severe acute respiratory distress syndrome, with $PaO_2 / FiO_2 = 86$ and bilateral infiltrates on the chest radiography. She was placed under mechanical ventilation in a pressure support mode with Positive End Expiration Pressure of 7cmH₂O. The doppler echocardiography showed pulmonary hypertension. The systolic pulmonary artery pressure estimated by the tricuspid regurgitation was measured at 53 mmHg compared to a normal value in children of ≤ 35 mmHg (35). There were no visible shunts, no valvulopathies, and no other obvious causes of pulmonary hypertension. After 6 days, the echocardiography values was normalized and extubation was performed after 9 days. The Oseltamivir treatment was stopped after five days since all bacteriological and viral sputum culture were negative. After ten days, the therapy was modified because of the clinical aggravation and cefotaxime and erythromycin were added to the vancomycin and stopped ceftriaxone and roxithromycin. Serological tests for *Mycoplasma pneumoniae* and *Chlamydia trachomatis* were negative. The child's condition improved and she went home after 20 days of hospitalization in total.

The evolution was characterized by an abnormal CT with pulmonary lesions 6 months later. She was treated for wheezes and coughing with fluticasone/salmeterol and

montelukast sodium. Since then, no other viral infections have occurred. P has been vaccinated and is seropositive for diphtheria, tetanus, pertussis, polio, *Haemophilus influenzae* type b (DTCP-Hib), hepatitis B virus, measles virus, mumps virus, rubella, *Streptococcus pneumoniae* (Prevnar) and *Neisseria meningitidis* group C (Meningitec). Additionally, P is seropositive for the following viruses without vaccination: human herpesvirus 6, human cytomegalovirus, varicella zoster virus, respiratory syncytial virus, adenovirus, and human parainfluenza viruses 1, 2 and 3. She is seronegative for EBV and HSV-1.

Materials and Methods

Whole Exome sequencing

Exome capture was performed with the SureSelect Human All Exon 50 Mb kit (Agilent Technologies). Paired-end sequencing was performed on a HiSeq 2000 (Illumina) generating 100-base reads. We aligned the sequences with the GRCh39 reference build of the human genome using the BWA aligner (36). Downstream processing and variant calling were performed with the Genome Analysis Toolkit (37), SAMtools (38), and Picard. Substitution and InDel calls were made with GATK Unified Genotyper. All variants were annotated using an annotation software system that was developed in-house (39-41).

Genetics

WES analysis of the trio (P and her parents) revealed a total of 18,426 variants in P. We filtered out all variations found in 1000 genomes database, dbSNP, our own database of 1,661 exomes for infectious diseases other than influenza, and variants found in the NHLBI-ESP6500 database at a frequency of >1%, leaving 144 non-synonymous coding variants in the patient's exome: 2 homozygous and 142 heterozygous, which include 3 genes with two compound heterozygous variants each, and seven *de novo* variants (Table S6). The heterozygous variants inherited from one parent were not considered in a model of complete penetrance. The homozygous, *de novo*, and two of the compound heterozygous variants affected genes unrelated to immunity, lungs or leukocytes (Table S7). The two mutated IRF7 alleles were not found in 1,046 gDNA samples from 52 ethnic groups (including French) from the HGDP-CEPH Human Diversity Panel. The missense F410V mutation had a CADD score of 14.25.

A genomic measure of individual homozygosity was plotted for P, two European individuals from consanguineous families, and 37 individuals from non-consanguineous families from our in-house WES database. Homozygosity was computed as the proportion of the autosomal genome belonging to runs of homozygosity (ROHs). The ROHs were defined as ranging at least 1 Mb of length and containing at least 100 SNPs, and were estimated using the *homozyg* option of the PLINK software (42). The centromeres were excluded because they are long genomic stretches devoid of SNPs and their inclusion might inflate estimates of homozygosity if both flanking SNPs are homozygous. The length of the autosomal genome was fixed at 2,673,768 kbs as previously described (43).

We estimated the selective pressure acting on *IRF7* to be 0.495 (indicative of purifying selection), by estimating the neutrality index (*NI*) (44) at the population level: $(P_N/P_S)/(D_N/D_S)$, where P_N and P_S are the number of non-synonymous and synonymous alleles, respectively, at population level (1000 Genomes Project) and D_N and D_S are the

number of non-synonymous and synonymous fixed sites, respectively, for the coding sequence of *IRF7*.

Cells

SV40-immortalized dermal fibroblasts, HEK293T, and Vero E6 cells were maintained in Dulbecco's modified Eagle medium (DMEM) supplemented with 10% fetal bovine serum. Stably-transfected dermal fibroblasts were obtained by transfecting pTRIP-IRF7iresRFP using Lipofectamine 2000 (Invitrogen, Carlsbad, CA, USA) according to the manufacturer's protocol. Stable transfectants were selected by puromycin treatment (0.4ug/mL) and subsequent fluorescence activated cell sorting for RFP-expressing cells yielding >80% RFP+ fibroblasts.

Peripheral blood mononuclear cells (PBMCs) were isolated on ficoll density gradient from whole blood collected in heparin-treated tubes from patient or healthy donors. PDCs/MDCs subsets were obtained from PBMCs of patient, her parents and healthy volunteers, by fluorescence-activated cell sorting (FACS) (BD FACS Aria II). PBMCs were thawed, washed and labeled with PerCP-conjugated anti-HLA-DR antibody (L243, BD Biosciences, San Diego, CA, USA); PECy7-conjugated anti-CD16 (3G8, mouse IgG1, BD Pharmingen), PacificBlue-conjugated anti-CD14 antibody (M5E2, BD Pharmingen), APC-conjugated anti-CD11c antibody (S-HCL-3, BD Biosciences), FITC-conjugated anti-BDCA2(CD303) antibody (AC144, Miltenyi Biotech, Germany), and PE-conjugated anti-CD3 (UCHT1, BD Biosciences), anti-CD15 (VIMC6, Miltenyi Biotech), anti-CD19 (4GT, BD Biosciences), anti-CD56 (MY31, BD Biosciences) and anti-NKp46 (BAB281, Beckman Coulter Immunotech, France) antibodies.

PDCs were sorted as HLA-DR⁺ BDCA2⁺ CD11c⁻ CD16⁻ CD14⁻ Lin (CD3, CD15, CD19, CD56, NKp46)⁻. Sorted cells were analysed for purity ($\geq 99\%$). Cells were dispensed in a 96-well round-bottom plate at a density of 1×10^4 cells/well, and cultured for 24h in OptiMem medium (Gibco) supplemented with 10% Fetal Bovine Serum (Gibco), 1% Penicillin-Streptomycin (Sigma), plus 10ng/ml IL-3 (R&D Systems) for PDCs, at 37°C in a 5% CO₂ atmosphere.

MDCs were sorted as HLA-DR⁺ CD11c⁺ BDCA2⁻ CD16⁻ CD14⁻ Lin(CD3, CD15, CD19, CD56, NKp46)⁻. Sorted cells were analyzed for purity ($\geq 99\%$). Cells were dispensed in a 96-well round-bottom plate at a density of 1.5×10^4 cells/well, and cultured for 24h in OptiMem medium (Gibco) supplemented with 10% Fetal Bovine Serum (Gibco), 1% Penicillin-Streptomycin (Sigma), plus 25ng/ml GM-CSF (R&D Systems) for MDCs, at 37°C in a 5% CO₂ atmosphere.

Primary dermal fibroblasts from P were reprogrammed to become induced pluripotent stem cells (iPSCs) by infection with non-integrating CytoTune Sendai viral vector kit (Life Technologies). Primary fibroblasts were plated in 12 well dishes at 50-80% confluency and transduced with the recombinant vectors according to manufacturer's protocol. Medium was changed after 24 hours of infection and the cells were allowed to grow for 6 days. On day 7, the cells were replated onto mouse embryonic fibroblast feeder cells. Medium was changed to iPS medium on day 8 and the cells were cultured until colonies formed. Reprogrammed cells were karyotyped to ensure genomic integrity.

Pulmonary epithelial cells were derived from embryonic or induced pluripotent stem cells as previously described (28). Briefly, hPSCs were passaged on Matrigel-coated plates for 12–24 h to deplete residual mouse embryonic fibroblasts before starting a differentiation

experiment. The differentiation began with primitive streak induction that started at day 0, performed in serum-free medium (SFD) containing 10 μ M Y-27632 and 3 ng/ml human BMP4. Definitive endoderm (DE) induction starts on day 1 and takes 3-3.5 days for reported hiPSCs. DE induction medium contains 10 μ M Y-27632, 0.5 ng/ml human BMP4, 2.5 ng/ml human bFGF and 100 ng/ml human Activin A for 72 or 84 h on low-adherence plates. Both primitive streak and DE inductions were performed in a 6-well Ultra-Low Attachment plate to form embryoid bodies (EBs). On day 4 or 4.5, EBs are dissociated with trypsin into single cells and plated onto 24-well fibronectin-coated tissue culture plates for anterior foregut endoderm (AFE) induction and subsequent lung progenitor induction. For day 4/4.5 to 6/6.5 AFE induction, cells were cultured in the presence of 1.5 μ M Dorsomorphin dihydrochloride (BMP signaling antagonist) and 10 μ M SB431542 (TGF- β signaling antagonist) for 24 h, and then switched to 24 h of 10 μ M SB431542 and 1 μ M IWP2 treatment. Day 6/6.5 to 15 lung progenitor induction medium contains 3 μ M CHIR99021 (WNT signaling agonist), 10 ng/ml human FGF10, 10 ng/ml human FGF7, 10 ng/ml human BMP4 and 50nM all-*trans* retinoic acid (ATRA). On day ~15 of differentiation, the lung field progenitor cell clumps were replated after brief trypsinization onto fibronectin-coated plates at 1:3 dilution. Day 15 to 25 cells were cultured in the presence of three factors (CHIR99021, 3 μ M, human FGF10, 10 ng/ml; human FGF7, 10 ng/ml). From day 25 to 55, cultures were carried further in the presence of these three factors with the addition of maturation components containing 50 nM dexamethasone, 0.1 mM (Sigma) 8-bromo-cAMP (Sigma) and 0.1 mM IBMX (3,7-dihydro-1-methyl-3-(2-methylpropyl)-1*H*-purine-2,6-dione) (Sigma). All the cytokines are from R&D Systems, all the small molecules are from Tocris (R&D Systems)

Plasmids

The cDNA of IRF7 was HA- or FLAG-tagged and cloned into pGEMT cloning vector (Promega, Madison, WI, USA). Site-directed mutagenesis was performed to obtain the indicated mutant constructs. All IRF7 constructs were subcloned into the pCAGGS vector for overexpression studies. IRF7 was cloned into the pTRIP.CMV.IV.Sb.ires.TagRFP_Dest vector using Gateway cloning technology (Life Technologies).

Western blotting and immunoprecipitation

Fibroblasts and pulmonary lung epithelial cells were pretreated with IFN- α 2b (Schering, Kenilworth, NJ, USA), IFN- β (PBL, Piscataway, NJ, USA), or IFN- λ (Prospec) for 18h prior to lysis. Cells were lysed in NP40 lysis buffer (280mM NaCl, 50mM Tris pH 8, 0.2mM EDTA, 2mM EGTA, 10% glycerol, 0.5% NP40) supplemented with 1mM DTT, 5mM Na₃VO₄ and Complete protease inhibitor cocktail (Roche, Mannheim, Germany). Protein lysate was resolved by SDS-PAGE and transferred to polyvinylidene fluoride (PVDF) membrane, which was probed with unconjugated primary antibodies and HRP-conjugated secondary antibodies. Anti-GAPDH (Santa Cruz) or anti- β -tubulin (Sigma-Aldrich, St. Louis, MO) antibodies are used as loading controls. IRF7 was probed with antibody recognizing the amino-terminus or phospho-IRF7 (Cell Signaling, Danvers, MA) at a dilution of 1:1000. RIG-I and IRF3 were levels were analyzed in fibroblasts as controls for IFN-dependent and -independent expression, respectively. FLAG-tagged IRF7 was precipitated using anti-FLAG M2 resin. Beads were extensively washed and resolved on SDS-PAGE and transferred as above. Blots were probed with anti-FLAG and -HA antibodies (Sigma-Aldrich).

Reporter assays

HEK293T cells were transfected with the indicated expression plasmids, firefly luciferase plasmids under the control of IFN- β , IFN- α 4 promoters, induced early after infection, or the IFN- α 6 promoter which is induced later in infection (11), and a constitutively expressing Renilla firefly luciferase plasmid for normalization. Twenty-four hours post-transfection, the cells were infected with 5 HA units of Sendai virus Cantell strain stock containing high amounts of defective interfering particles, a strong type I IFN inducer (45), for 18 hours. Luciferase levels were measured using Dual-Glo reagent according to the manufacturer's protocol (Promega, Madison, WI). Firefly luciferase values are normalized to Renilla luciferase values and fold induction is expressed relative to the empty vector transfected sample. Statistical significance was determined by two-tailed paired t-tests.

Microscopy

Vero cells were grown on glass cover slips coated with poly-L-lysine (Invitrogen) and transfected with plasmids encoding IRF7 WT, F410V or Q421X by Lipofectamine 2000 (Invitrogen). Twenty-four hours post-transfection, the cells were infected with 5 HA units of Sendai virus Cantell strain. Eight hours post-infection, the cells were fixed with 4% paraformaldehyde and stained with mouse anti-FLAG antibody (Sigma-Aldrich) at a dilution of 1:400 and an anti-mouse Alexa 568 conjugated secondary antibody (Molecular Probes) at a concentration of 1 μ g/mL. Nuclear DNA was stained with Hoechst 33342 at a concentration of 0.1 μ g/mL. Images were acquired on an Axioplan 2 imaging upright widefield epifluorescence microscope (Zeiss).

Pulmonary epithelial cultures were stained at day 55 with positive and negative biological staining controls as previously described (28). After influenza infection, the cells were fixed with 4% paraformaldehyde, washed with PBS, permeabilized with 0.25% Triton and 5% normal donkey serum (Jackson ImmunoResearch, West Grove, PA), and blocked in 5% normal donkey serum. The cell cultures were stained with a combination of the following primary antibodies: TTF-1/Nkx2.1 (Rabbit, Seven Hills Bioreagents, Cincinnati, OH) and influenza A NP (HT103 mouse antibody) in 5% normal donkey serum in PBS at 4°C overnight. The cultures were then incubated with donkey anti-mouse whole IgG-Alexa Fluor 488 (Jackson ImmunoResearch) and donkey anti-rabbit whole IgG-Cy3 (Jackson ImmunoResearch) at 1:300 dilutions in 5% normal donkey serum at room temperature for 2 h, washed twice and incubated with DAPI for 5 min at room temperature. The stained cultures were preserved in VECTASHIELD Mounting Media (Vector laboratories, Inc. Burlingame, CA) in dark at 4 °C.

Samples were imaged using motorized Leica DMI 6000B fluorescence microscope coupled with Leica DFC365 FX digital camera and operated by LAS AF 6.2 software (Leica Microsystems GmbH, Wetzlar, Germany). All images were acquired with HCX PL S-APO 10 \times /NA 0.3 or HCX PL FL L 20 \times /NA 0.4 objectives. The tile scan images were taken with the image tiling module coupled with either autofocus or z-stack scanning (1.5 μ m/stack) module, and auto-stitched by the LAS AF 6.2 software. The images were exported as JPG files and processed (contrast and brightness adjustments) with Photoshop CS5.1 (Adobe Systems, San Jose, CA). Cell scoring of influenza NP⁺ Nkx2.1⁺ pulmonary epithelial cells was performed using the Cell Scoring Module of MetaMorph Image Analysis Software (Molecular Devices, Sunnyvale, CA, USA). 'Controls' comprise the mean of RUES2 and SV-iPSC derived pulmonary epithelial cells

and ‘patient’ comprises cells derived from three independent clones of P’s iPSCs. Total number of untreated cells scored for controls was 167,293 and for patient was 219,293. Data points are colored to indicate the genotype of the ESC/iPSC. Statistical significance was determined using a Chi-square test.

Cell stimulation assays

SV40-fibroblasts were plated at a density of 10^5 cells per well in 24-well dish and incubated overnight. Polyinosinic-polycytidylic acid (poly(I:C); Amersham, Piscataway, NJ) was added to the culture medium at a concentration of 25 μ g/mL or the cells were transfected with 2.5 μ g of poly(I:C) using Lipofectamine 2000 (Invitrogen, Carlsbad, CA) according to manufacturer’s protocol. Fibroblasts were stimulated by infection with 5 HA units of Sendai virus or VSV, hPIV3, influenza A/CA/4/2009 or A/PR/8/34-GFP at MOI=1. Culture medium was harvested after 24h of stimulation or infection and IFN- β was measured by ELISA. Pulmonary epithelial cultures were stimulated by infection with influenza A/PR/8/34 at MOI=0.1 and IFN- β was measured by ELISA. Statistical significance was determined by individual t-test.

PBMCs from healthy controls, P and her parents were cultured in 10 μ g/mL polymyxin B and infected at a density of 2e6 cells/mL with the following viruses herpes simplex virus 1 (HSV-1) at MOI=1, BK virus at MOI=0.5, VSV WT and M51R mutant (46) at MOI=1, Newcastle Disease virus (NDV) at MOI=0.5, Mumps virus at MOI=0.05, Measles virus at MOI=0.002, Sendai virus at MOI=10, human parainfluenza virus 3 (Para III) at MOI=0.05, Sindbis virus at MOI=0.2, and encephalomyocarditis virus (EMCV) at MOI=0.5. 24 hours post-infection, supernatants were collected and cytokines were measured by ELISA according to the manufacturer’s protocol.

Virus assays

Hemagglutination inhibition assay. The patient’s serum samples were treated with trypsin-heat-periodate to remove non-specific inhibitors to hemagglutination as previously described (47). Briefly, one volume of sera was mixed with half a volume of receptor destroying enzyme, trypsin 8 mg/ml (Sigma-Aldrich, St. Louis, MO) in 0.1 M phosphate buffer, pH 8.2 and then incubated for 18h at 37°C. The trypsin was inactivated by incubation of the sera for 30 min at 56°C. The samples were allowed to cool to room temperature (RT) and were mixed with 3 volumes of 0.11 M metapotassium periodate and incubated at room temperature (RT) for 15 min. Three volumes of 1% glycerol saline were then added and mixed with the samples and further incubated for 15 min at RT. The samples were mixed with 2.5 volumes of 0.85% saline resulting in final testing dilution of 1:10. The viruses used for the HI assay were A/Netherlands/602/2009, Perth/16/2009/H3N2, B/Brisbane/60/48. HI assays of virus and sera were conducted following standard protocols (48). Two-fold serial dilutions of sera were mixed and pre-incubated in Nunc V-bottom 96-well microtiter plates (Nalge Nunc International, Rochester, NY) for 30 min at 4°C with 4 HA units of virus per well. Turkey red blood cells were added to a final concentration of 0.5%, and the plate was incubated on ice for 30 min. Hemagglutination inhibition (HI) titers of sera were determined as the inverse of the last dilution where cells were not agglutinated.

Virus replication. SV40-fibroblasts were infected with influenza virus (A/Netherlands/602/2009) at a multiplicity of infection (MOI) of 10 (MOI=10). Pulmonary epithelial cells were infected with influenza virus (A/CA/4/2009) at MOI=1.

The inoculum was absorbed onto the cells for 30 minutes at 25°C, cells were washed twice with PBS and cultured at 37°C in the presence of 0.1 or 1 µg/mL TPCK-trypsin (Sigma-Aldrich, St. Louis, MO, USA) for fibroblasts and pulmonary epithelial cells, respectively. Virus samples were collected at the indicated times after infection. Influenza titers were determined by plaque assay on Madin –Darby canine kidney cells (MDCK) cells. Fibroblasts were infected with vesicular stomatitis virus (VSV) at MOI=3. The inoculum was absorbed onto the cells for 30 minutes at 25°C, washed twice with PBS and cultured in DMEM 10% FBS at 37°C. Virus samples were collected at indicated time points. Viral titers were determined by endpoint dilution on Vero cells using the Reed and Muench calculation. Where indicated, cells were pretreated with IFN- α 2b (Schering, Kenilworth, NJ, USA), IFN- β (PBL, Piscataway, NJ, USA), or IFN- λ (Prospec) for 18h prior to virus infection. Statistical significance was determined by individual t-tests.

Quantitative RT-PCR

RNA was isolated from SV40-fibroblasts and B-EBV cells were stimulated with 1,000 IU/mL IFN- β (PBL, Piscataway, NJ) for 4, 6, or 8h with TRIzol according to manufacturer's protocol (Invitrogen, Carlsbad, CA). The RNA was DNase-treated (Roche, Mannheim, Germany) cleaned by passage through RNeasy column (Qiagen). Reverse transcriptase PCR was performed using random hexamers according to the manufacturer (Applied Biosystems, Foster City, CA). Quantitative real-time PCR (qPCR) was performed with Applied Biosystems Taqman assays using the β -glucuronidase (GUS) housekeeping gene for normalization. Results are expressed using the $\Delta\Delta C_t$ method, as described by the manufacturer. Sanger sequencing of the *IRF7* cDNA showed both alleles, suggesting that there was little nonsense-mediated decay of the Q421X mRNA

Microarray

Data acquisition. PBMC from patient and controls were infected with influenza A/CA/4/2009 at MOI=2 for 8 or 16 hours or left unstimulated for the same amount of time. Total RNA was isolated (RNeasy kit; QIAGEN) and RNA integrity was assessed on an Agilent 2100 Bioanalyzer (Agilent Technologies). Biotinylated cRNA targets were prepared from 250 ng of total RNA, using the Illumina TotalPrep RNA Amplification kit (Ambion). The labeled cRNAs (750 ng) were then incubated for 16h to HT-12 version 4 BeadArrays (48,323 probes). BeadChip arrays were then washed, stained, and scanned on a HiScanSQ (Illumina) according to the manufacturer's instructions.

Data preprocessing. Only the probes called present in at least one sample ($P < 0.01$) were retained for downstream analysis ($n = 20,517$). We then performed internal trimmed means normalization (49) for the patients and controls samples, separately for the 8h and 16h time points.

Data analysis. For each time point we calculated for each individual the fold change (FC) between unstimulated and stimulated conditions. We finally selected the probes with 10% highest FC between the patients and median of the controls ($n=100$), and plotted with a heatmap of hierarchically clustered probes using the `gplots` package of the R statistical programming language (<http://cran.r-project.org/web/packages/gplots/>). We further analyzed these probes using the Causal Network Analysis package from Ingenuity Pathway Analysis.

Figure S1. Patient's serology for influenza and other viruses. (A and B) Serum from P, drawn at indicated dates, was measured for the ability to inhibit the hemagglutination of chicken red blood cells by the indicated influenza viruses. Hemagglutination inhibition (HAI) indicates the presence of neutralizing antibodies. Data are presented as the reciprocal of the highest dilution of serum with neutralizing activity. (C) P's seropositivity for common viruses in childhood as taken from clinical and laboratory reports.

Figure S2. Sanger sequencing confirmation of *IRF7* mutations found by WES. (A) A genomic measure of individual homozygosity was plotted for P, two European individuals from consanguineous families, and 37 individuals from non-consanguineous families. Homozygosity was computed as the proportion of the autosomal genome belonging to runs of homozygosity (ROHs). (B) Electropherogram traces at the two loci in *IRF7* harboring heterozygous mutations. The patient and father are heterozygous for c.1228T>G/T (F410V) and the patient and mother are heterozygous for c.1261C>T/C (Q421X). Heterozygous calls are denoted by K (T/G) and Y (C/T).

Figure S3. Functional assay for other *IRF7* variants found in WES database.

Luciferase reporter assays for *IFNB* and *IFNA4* promoters in HEK293T cells expressing *IRF7* variants found in our in-house WES database. Cells are uninfected (UI) or infected with Sendai virus Cantell strain (SeV). Induction is shown relative to uninfected empty vector transfected cells and normalized to Renilla luciferase values. The mean of three independent experiments is shown with error bars indicating the SD.

Figure S4. Assessing the dominant negativity of F410V and Q421X alleles. (A) Constructs expressing the two mutant alleles were cotransfected into 293Ts with *IFNB* and *IFNA6* reporter constructs. Twenty-four hours post-transfection, the cells were left uninfected or infected with Sendai virus. Luciferase values were read 24hpi and are normalized to the expression in uninfected empty vector (EV)-transfected cells. Error bars indicate SD. (B) The *IFNA6* reporter assay was performed as in (A). WT *IRF7* was transfected at 1 μ g with 1, 2 or 3 μ g of constructs expressing the mutant alleles. A previously described dominant negative expressing amino acids 247-503 (50) was included as positive control for inhibition of WT and GST served as negative control. (C) To determine whether the mutant alleles of *IRF7* interact with *IRF3*, FLAG-*IRF7* and HA-*IRF3* were cotransfected in 293Ts. *IRF7* was immunoprecipitated from the lysates with anti-FLAG antibody and WB was performed with FLAG, HA and GAPDH antibodies. (D) *IFNB* reporter assay was performed as in (B) with 1 μ g *IRF3* cotransfected with increasing amounts of WT-*IRF7* (*IRF7*), F410V and Q421X. GST was included as negative control.

Figure S5. Genome-wide expression levels in uninfected PBMCs. The log₂ fold change (FC) between P and the mean of the healthy donors in uninfected PBMCs. The differential gene expression is significantly enriched for immune response genes ($p=2.8e-21$).

Figure S6. Cytokine responses from P's PBMCs infected with viruses or treated with TLR ligands. PBMCs were isolated from the blood of a healthy control, the patient, her father and her mother, and stimulated with the indicated viruses. Supernatants were

harvested 24h post-treatment and IFN- α 2, IFN- β , IL-29 and IL-6 were measured by ELISA.

Figure S7. IFN response of influenza infected pDCs. (A) Plasmacytoid DCs were isolated from the fresh blood of a healthy control, P and her mother. IFN- α 2 production was measured after infection with influenza A virus at MOI=1. pDCs and unsorted PBMCs were infected with influenza virus and (B) IFNL genes (IL29, IL28A and IL28B) and (C) *IRF7* and *MX1* expression levels were measured by qPCR at 8hpi. Data are relative to 18S expression and are representative of two independent experiments.

Figure S8. Influenza phenotype in P's fibroblasts. (A) SV40-transformed fibroblasts were infected with an H5N1 isolate of influenza virus. Titers were measured at indicated times post-infection. (B and C) SV40 fibroblasts were left untreated or treated with IFN- α 2b for 18h and then infected with VSV at MOI=3 or influenza at MOI=1. Titers were measured at indicated times post-infection. (D) Fibroblasts were infected with influenza PR/8 or PR/8-GFP in the presence of 0.1 μ g/mL TPCK-trypsin. IFN- β was measured by ELISA at 24h post-infection. (E) Left panel, Fibroblasts from the indicated individuals were stimulated with extracellular poly(I:C), transfected with lipofectamine (LPF) or treated with LPF alone. Right panel, Fibroblasts were infected with VSV WT, M51R mutant, human parainfluenza virus (hPIV3) at MOI=1 and 5 HA units of Sendai virus (SeV).

Figure S9. Exogenous IFN reduces influenza virus replication in pulmonary epithelial cells. Pulmonary epithelial cells derived from healthy ESCs and SV-iPSCs and three independent patient iPSC clones were left untreated or treated with 1,000U of IFN- α , 1,000U IFN- β or 0.1ng/mL IFN- λ for 18h and then infected with influenza virus A/CA/4/2009 for the indicated time points. Titers were measured by plaque assay on MDCK cells.

Table S1. pH1N1 WES data by age at infection. The 22 individuals analyzed are displayed by their age at the time of pH1N1 infection.

Table S2. Immunophenotyping of P leukocyte subsets. Patient values for the indicated leukocyte subsets are shown in comparison to reference values. T cell proliferation upon stimulation with the indicated antigen.

Table S3. Clinical phenotype of patients in WES database. The individuals subjected to WES are divided by the pathogen. HSE, herpes simplex encephalitis; MSMD, Mendelian susceptibility to mycobacterial disease; TB, Tuberculosis; CMC, chronic mucocutaneous candidiasis.

Table S4. IRF7 variants found in in-house WES database. Variants in IRF7 that were found by searching our in-house database of 1,661 exomes from non-influenza patients. Their impact on IRF7 as predicted by Poly-Phen2 and SIFT and their presence or absence in dbSNP are shown.

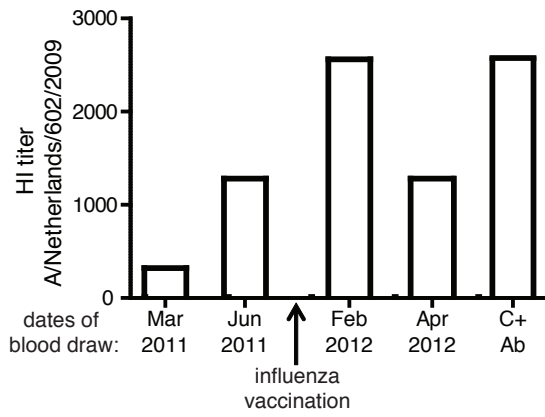
Table S5. pDC and mDC frequencies in P. The indicated frequencies of pDCs and mDCs isolated from P, an UNC-93B-/- individual who suffered from HSE and 6 healthy donors are shown. These data indicate normal numbers of each cell type in P.

Table S6. Unique variants found in P WES data. The total number of variants, homozygous or heterozygous, found in P. Variants found in 1000 Genomes, dbSNP, our in-house exome database from 1661 patients were filtered out as were variants found in the NHLBI-ESP6500 database at a frequency of >1%.

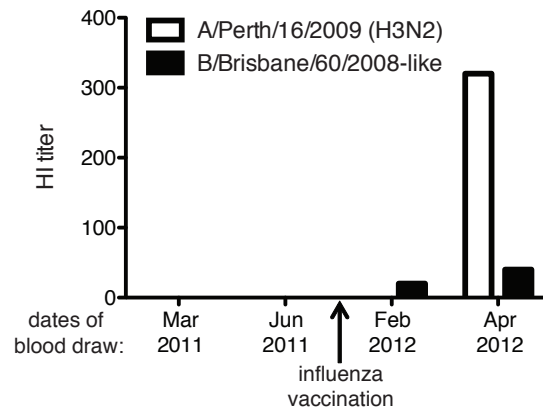
Table S7. Additional unique variants found in P WES data. The 2 compound heterozygous, 2 homozygous, and 9 *de novo* variations found in P alone with their chromosomal positions, Ensembl accession numbers, variation and CADD score.

Figure S1

A



B

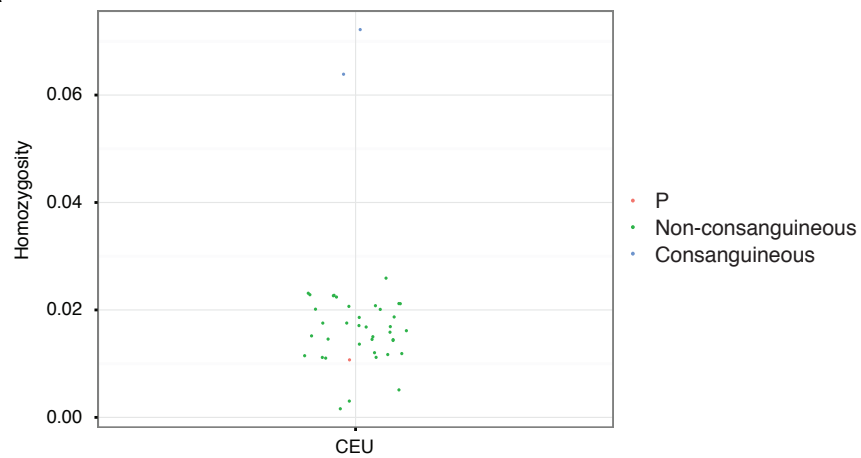


C

Virus	Seropositivity	Vaccination
Influenza A	Positive	Yes (after illness)
Influenza B	Weak positive	Yes (after illness)
Hepatitis A	Negative	No
Hepatitis B	Positive	Yes
Parvovirus	Negative	No
Respiratory syncytial virus	Positive	No
Adenovirus	Positive	No
Human parainfluenza virus 1	Positive	No
Human parainfluenza virus 2	Positive	No
Human parainfluenza virus 3	Positive	No
Measles	Positive	Yes
EBV	Negative	No
VZV	Positive	No
CMV	Positive	No
HSV	Negative	No

Figure S2

A



B

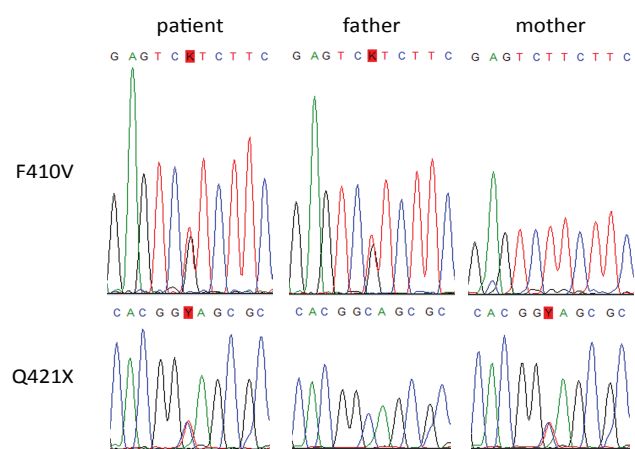


Figure S3

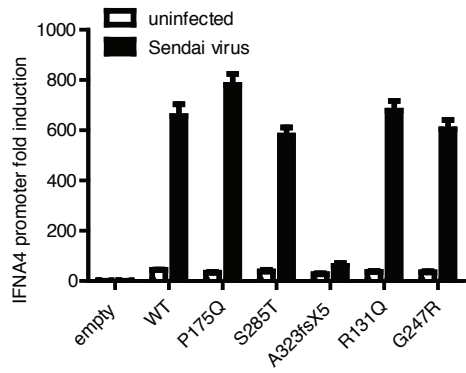
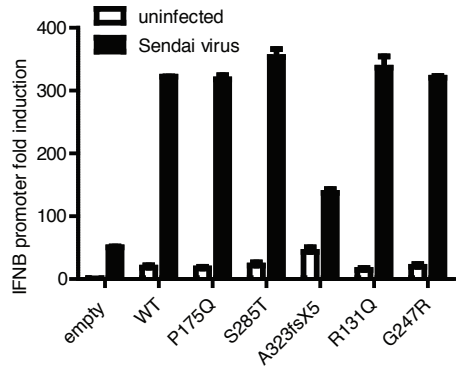
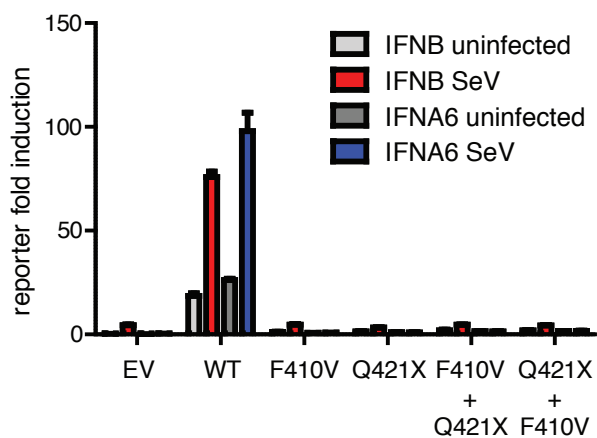
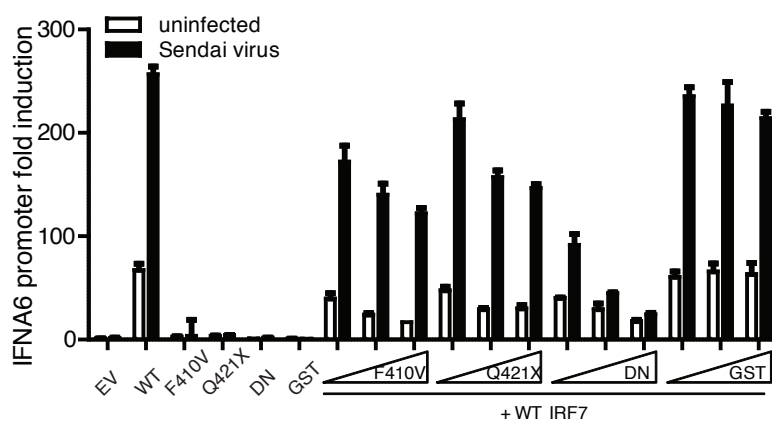


Figure S4

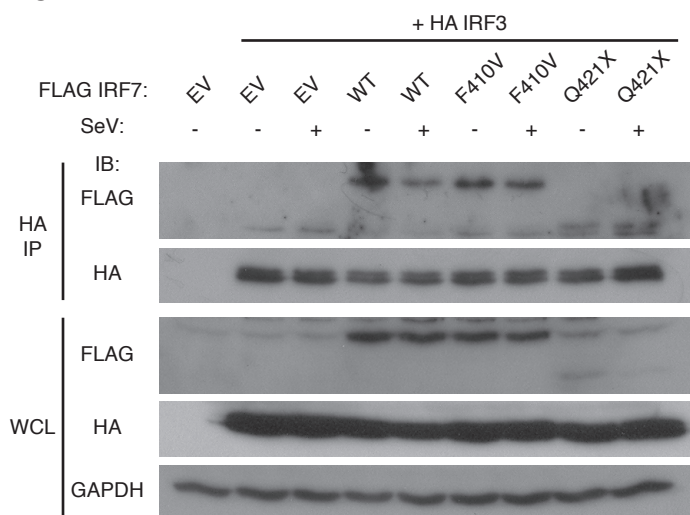
A



B



C



D

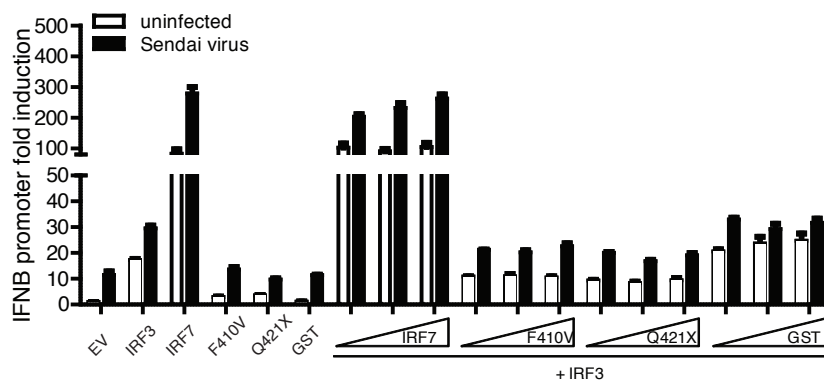


Figure S5

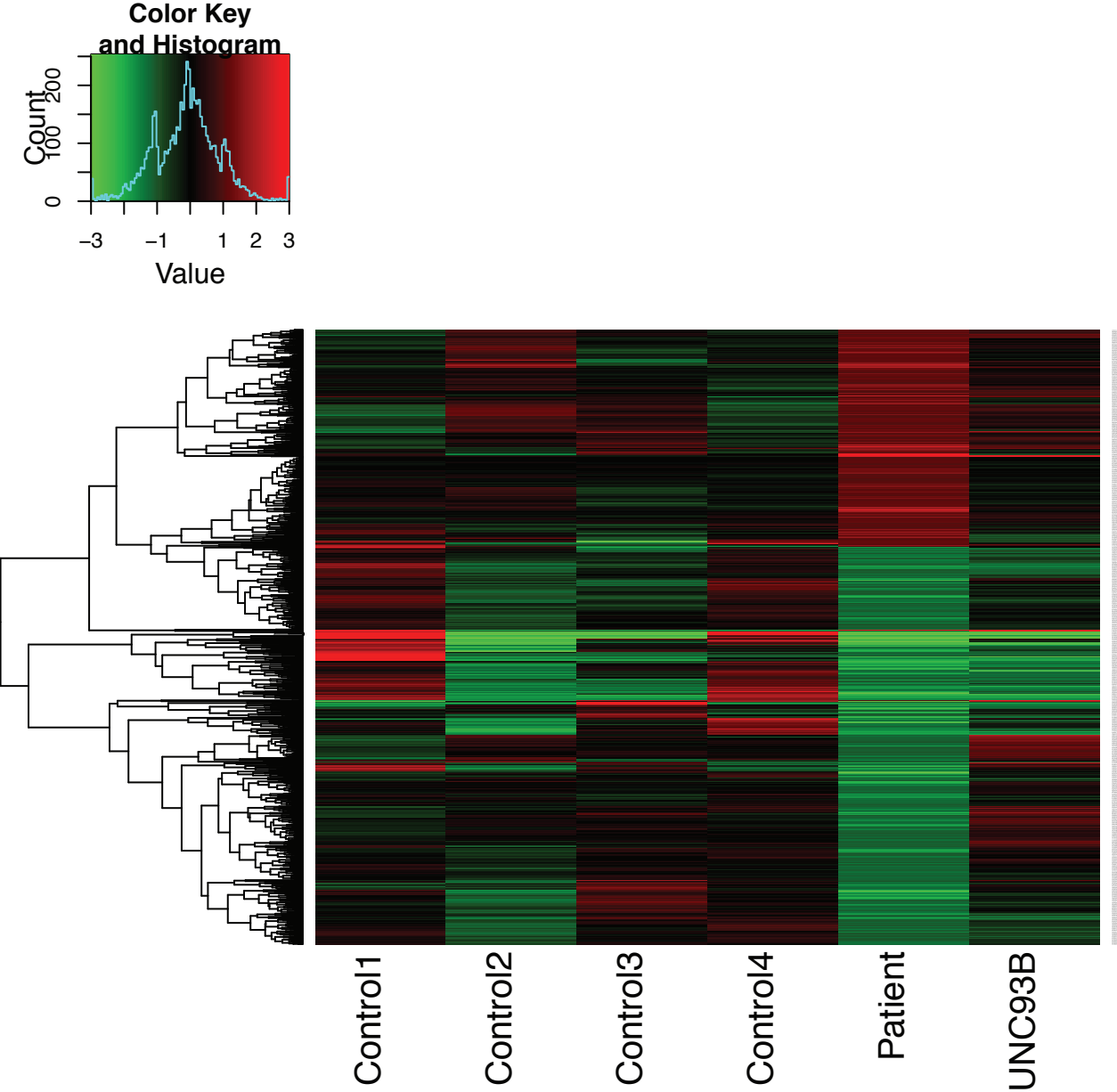
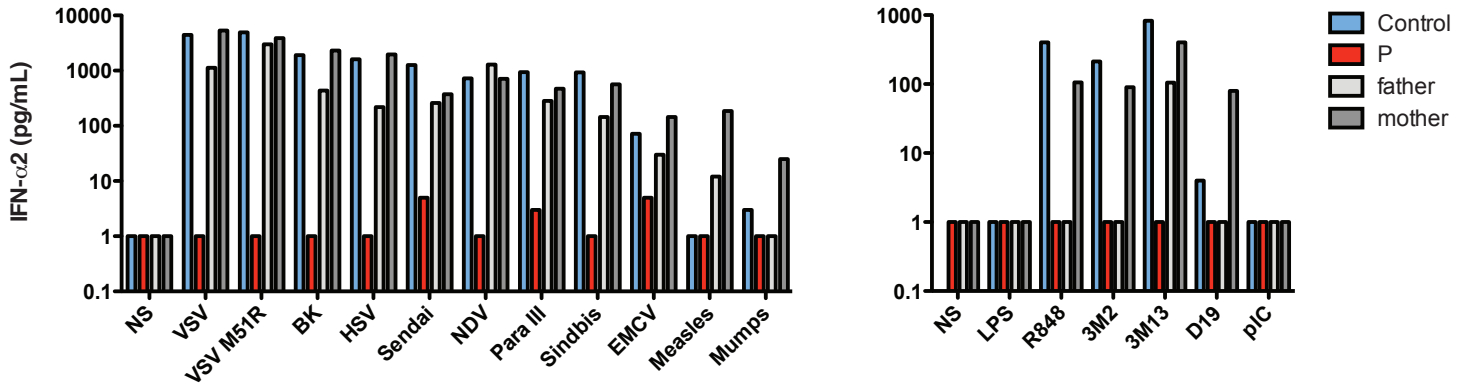
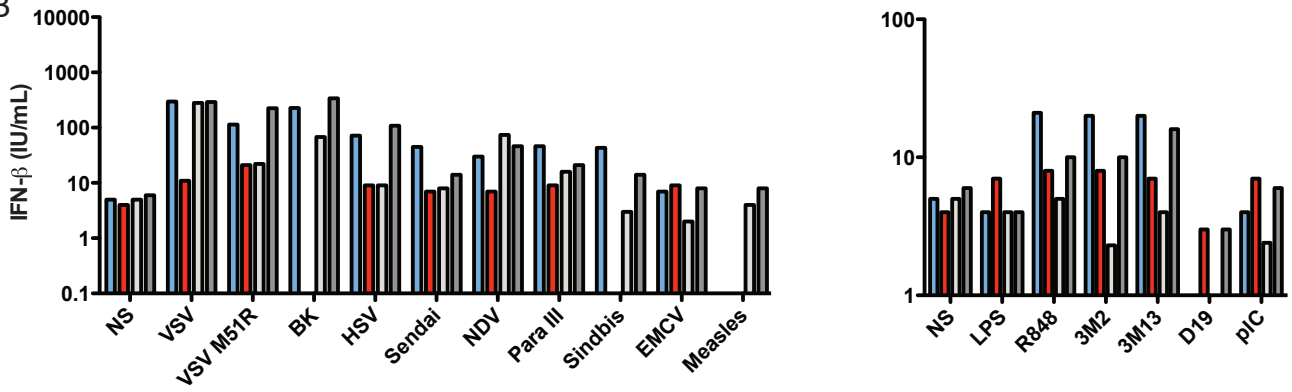


Figure S6

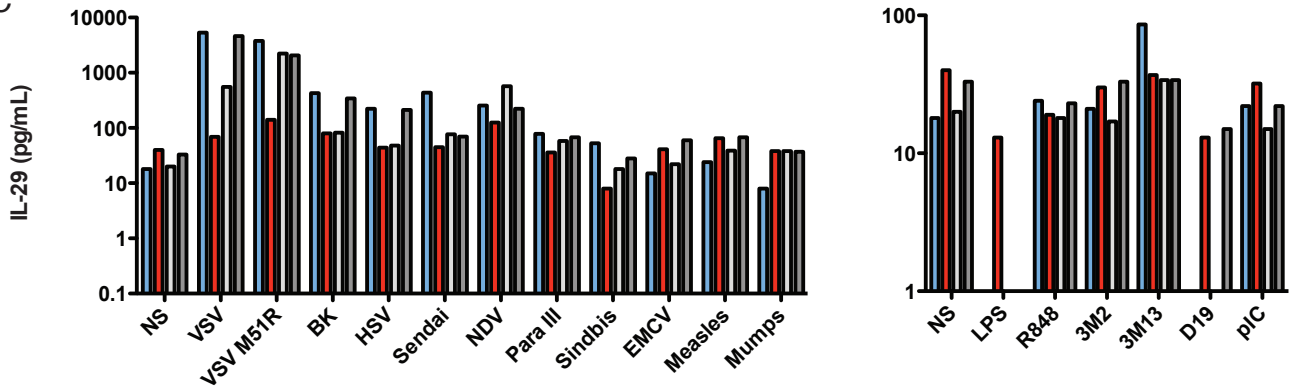
A



B



C



D

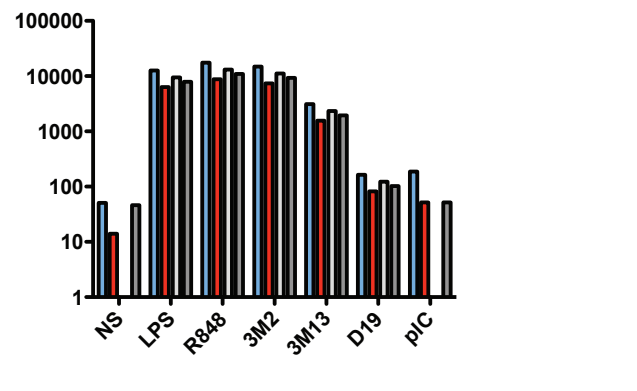
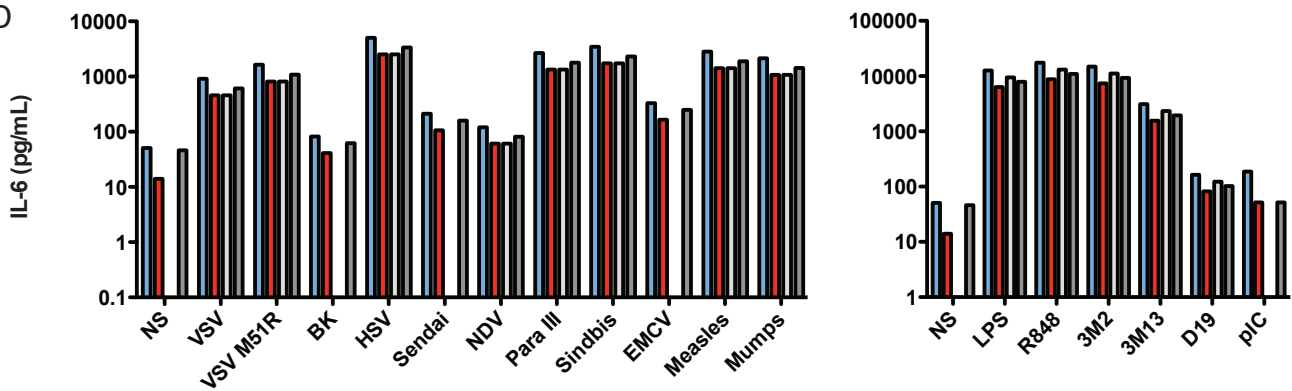
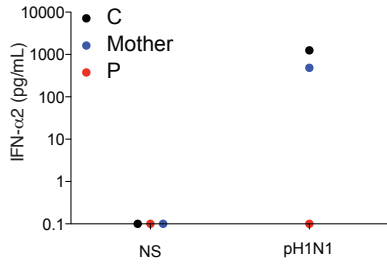
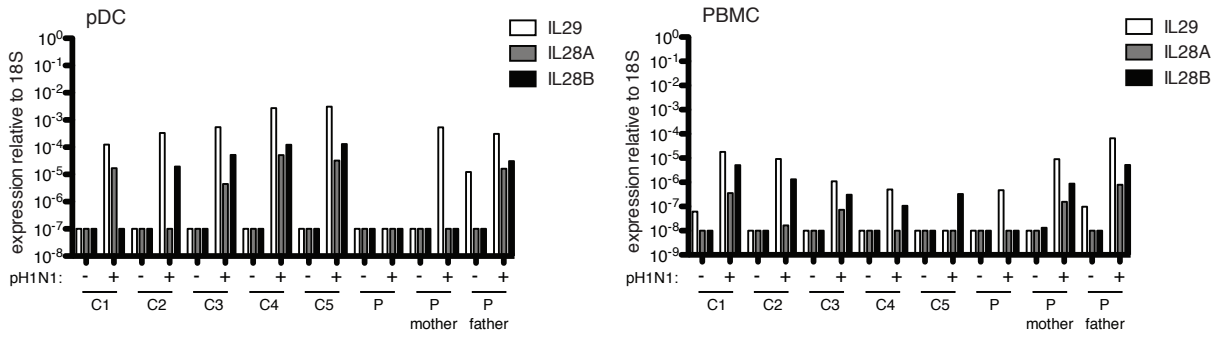


Figure S7

A



B



C

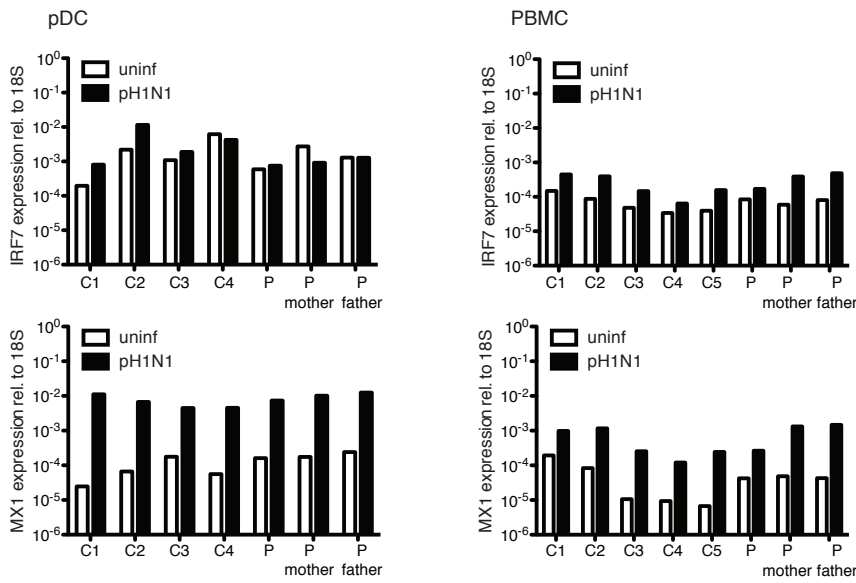
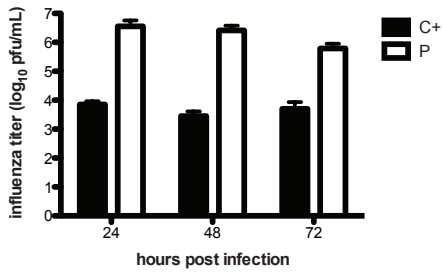
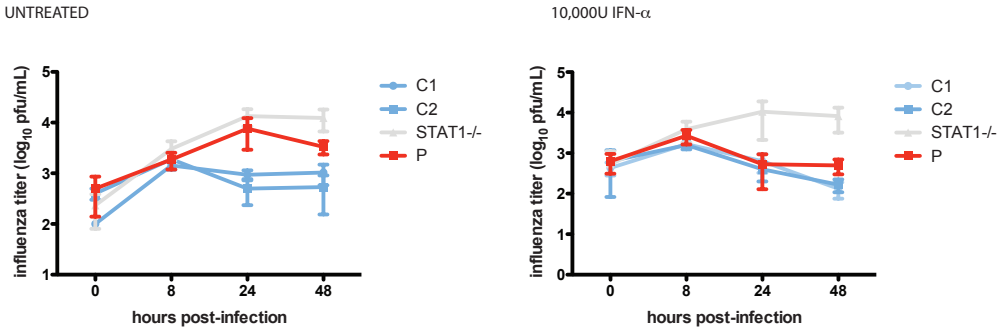


Figure S8

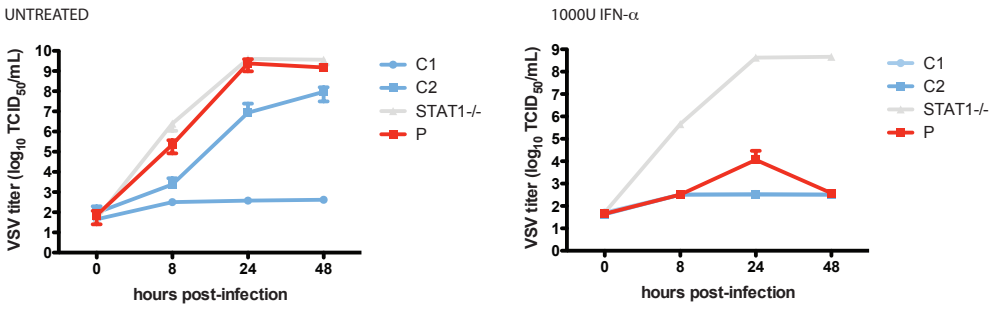
A



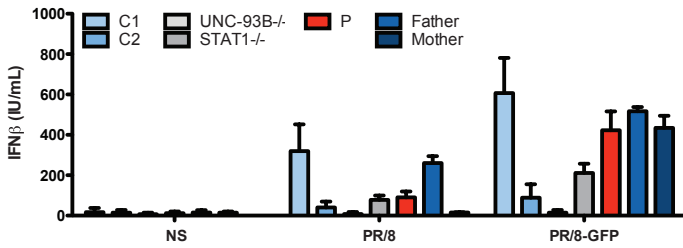
B



C



D



E

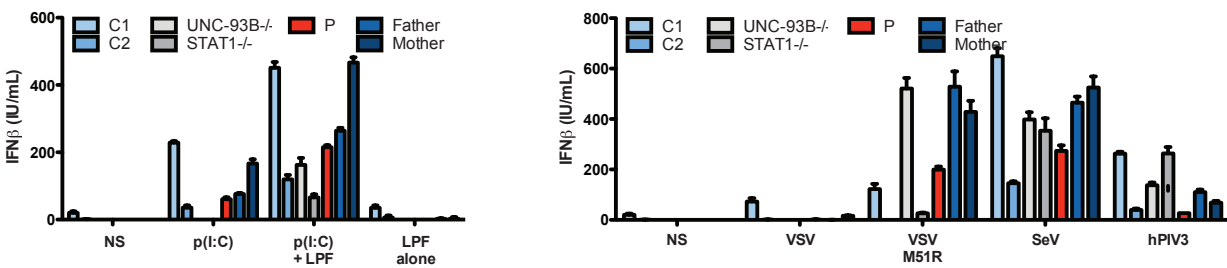


Figure S9

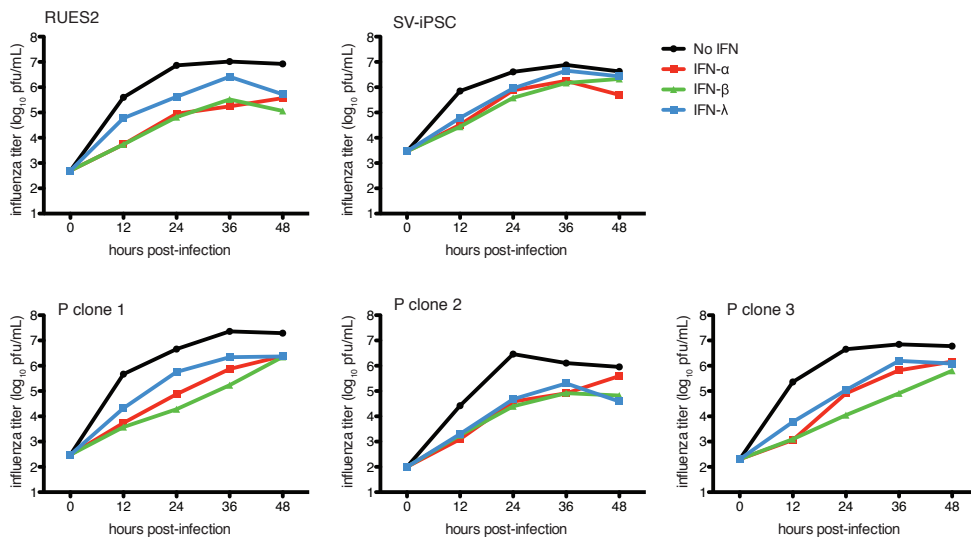


Table S1

Age	# of individuals
0-4	3
5-17	1
18-49	15
50-64	3
65+	0
total	22

Table S2**Immunophenotyping**

Parameter	Patient values	Median value for 2-5 years old*
Total lymphocytes (cells/ μ L)	3400	
T lymphocytes		
CD3+ (%)	80	60-76
CD3+	2720	1200-2600
CD4+ (%)	47	31-47
CD4+	1598	65-1500
CD8+ (%)	29	18-35
CD8+	986	370-1100
CD45RO+/CD4+ (%)	26	9-26
CD45RA+/CD4+ (%)	74	58-70
CD31+ CD45RA+/CD4+ (%)	48	43-55
CCR7+ CD45RA+/CD8+ (%)	43	52-68
CCR7+ CD45RA-/CD8+ (%)	4	3-4
CCR7- CD45RA-/CD8+ (%)	40	11-20
CCR7- CD45RA+/CD8+ (%)	14	16-28
B Lymphocytes		
CD19+ (%)	14	13-27
CD19	476	270-860
CD27+/CD19+ (%)	23	11.1-20.4
CD27-IgD+/CD19+ (%)	74	73.6-84.1
CD27+IgD-/CD19+ (%)	18	4.7-10.2
CD27+IgD-/CD19+ (%)	6	4.4-10.4
NK lymphocytes		
CD16+CD56+ (%)	6	4-17
CD16+CD56+	204	100-480

* Shearer et al 2003 Journal of Allergy and Clinical Immunology Vol 112, Number 6

Cell proliferation

Condition	Cell number (cpm/ 10^3)
nonstimulated (day 3)	1.9
PHA	85.8
non-stimulated (day 6)	1.7
Tetanus	2.4
Cytomegalovirus	14
Poliovirus	21.5

Table S3

Group (principal infectious disease of group)	number
Viral disease (HSE, influenza)	566
Mycobacterial disease (MSMD and TB)	515
Congenital asplenia	52
Fungal disease (CMC)	167
Pneumococcal infection	177
Staphylococcal infection	86
T and B cell immunodeficiencies	98
total	1661

Table S4

variant		zygosity	PolyPhen	SIFT	dbSNP
c.227G>A	p.G76E	het	0.019	0.02	n
c. 256G>T	p.A86S	het	0.036	0.31	n
c.273G>A	p.W91X	het	n/a	n/a	n
c.321G>T	p.M107I	het	0.129	0.25	n
c.392G>A	p.R131Q	het	0.197	tolerated	y
c.460C>A	p.P154T	het	0.026	tolerated	n
c.475C>A	p.L159M	het	0.905	0.01	n
c.524C>A	p.P175Q	het	0.505	tolerated	n
c.739G>A	p.G247R	het	0	tolerated	y
c.854G>C	p.S285T	het	0.05	tolerated	y
c.969delC	p.A323fsX5	het	n/a	n/a	n
c.1423A>T	p.S475C	het	0.921	d	n
c.1439T>A	p.L480H	het	0.998	d	n

Table S5

	pDCs as % of PBMCs (live cells, doublets excluded)	pDCs as % of HLA- DR+ Lineage- cells	mDCs as % PBMCs (live cells, doublets excluded)	mDCs as % of HLA- DR+ Lineage- cells
IRF7 patient	0.34	2.34	0.62	4.26
UNC93B Patient	0.43	3.82	0.76	6.73
Mean Ctrl (n=6)	0.28	1.34	0.51	2.64
Std Deviation	0.16	0.34	0.14	0.71

Table S6

Whole Exome Sequencing		# of variants
Nonsense (stop-gained)	Total	98
	Homozygous	0
	Heterozygous	4
Readthrough (stop-lost)	Total	57
	Homozygous	0
	Heterozygous	1
Missense	Total	5474
	Homozygous	2
	Heterozygous	130
Silent	Total	5480
	Homozygous	0
	Heterozygous	64
Frameshift	Total	132
	Homozygous	0
	Heterozygous	4
Inframe	Total	124
	Homozygous	0
	Heterozygous	3
UTR	Total	5108
	Homozygous	0
	Heterozygous	53
Splice	Total	1812
	Homozygous	0
	Heterozygous	20
ncRNA	Total	141
	Homozygous	0
	Heterozygous	0

Table S7

	CHROMOSOME	POSITION	GENE	TRANSCRIPT	MUTATION		CADD Phred
comp het	11	613094	IRF7	ENST00000397574	p.Q421X	c.C1261T	33.0
	11	613215	IRF7	ENST00000397574	p.F410V	c.T1228G	14.3
	17	40932763	WNK4	ENST00000591448	p.T16I	c.C47T	11.8
	17	40932954	WNK4	ENST00000591448	p.A80T	c.G238A	7.8
homozyg	11	1857428	SYT8	ENST00000535046	p.V158I	c.G472A	4.7
	18	8819075	SOGA2/MTCL1	ENST00000518815	p.M992V	c.A2974G	9.0
de novo	6	111346763	RPF2	ENST00000441448	p.S300X	c.899C>A	16.3
	11	1018170	MUC6	ENST00000421673	p.T1544K	c.4631C>A	8.6
	11	123900762	OR10G8	ENST00000431524	p.T145A	c.433A>G	0.0
	1	201178702	IGFN1	ENST00000335211	p.V1561M	c.4681G>A	9.7
	1	201178705	IGFN1	ENST00000335211	p.N1562D	c.4684A>G	7.3
	3	195505822	MUC4	ENST00000477086	p.P4210L	c.12629C>T	3.7
	19	42867205	MEGF8	ENST00000251268	p.T2022P	c.6064A>C	15.7
	10	23290935	ARMC3	ENST00000298032	p.M505L	c.1513A>C	6.0
	17	17697103	RAI1	ENST00000353383	p.Q841-	c.841_843delCAG	n/a

References

1. P. Palese, M. L. Shaw, in *Fields Virology*, D. Knipe, P. Howley, Eds. (Lippincott Williams & Wilkins, Philadelphia, ed. 5, 2007), pp. 1647–1689.
2. W.-J. Shieh, D. M. Blau, A. M. Denison, M. Deleon-Carnes, P. Adem, J. Bhatnagar, J. Sumner, L. Liu, M. Patel, B. Batten, P. Greer, T. Jones, C. Smith, J. Bartlett, J. Montague, E. White, D. Rollin, R. Gao, C. Seales, H. Jost, M. Metcalfe, C. S. Goldsmith, C. Humphrey, A. Schmitz, C. Drew, C. Paddock, T. M. Uyeki, S. R. Zaki, 2009 pandemic influenza A (H1N1): Pathology and pathogenesis of 100 fatal cases in the United States. *Am. J. Pathol.* **177**, 166–175 (2010). [Medline](#)
[doi:10.2353/ajpath.2010.100115](https://doi.org/10.2353/ajpath.2010.100115)
3. F. S. Dawood, L. Kamimoto, T. A. D’Mello, A. Reingold, K. Gershman, J. Meek, K. E. Arnold, M. Farley, P. Ryan, R. Lynfield, C. Morin, J. Baumbach, S. Zansky, N. Bennett, A. Thomas, W. Schaffner, D. Kirschke, L. Finelli, Children with asthma hospitalized with seasonal or pandemic influenza, 2003-2009. *Pediatrics* **128**, e27–e32 (2011).
[Medline](#) [doi:10.1542/peds.2010-3343](https://doi.org/10.1542/peds.2010-3343)
4. Centers for Disease Control and Prevention, FluView: Influenza-Associated Hospitalization Surveillance Network (2013); <http://gis.cdc.gov/grasp/fluview/FluHospChars.html>.
5. A. R. Gennery, A. J. Cant, Diagnosis of severe combined immunodeficiency. *J. Clin. Pathol.* **54**, 191–195 (2001). [Medline](#) [doi:10.1136/jcp.54.3.191](https://doi.org/10.1136/jcp.54.3.191)
6. W. Al-Herz, A. Bousfiha, J. L. Casanova, T. Chatila, M. E. Conley, C. Cunningham-Rundles, A. Etzioni, J. L. Franco, H. B. Gaspar, S. M. Holland, C. Klein, S. Nonoyama, H. D. Ochs, E. Oksenhendler, C. Picard, J. M. Puck, K. Sullivan, M. L. Tang, Primary immunodeficiency diseases: An update on the classification from the international union of immunological societies expert committee for primary immunodeficiency. *Front. Immunol.* **5**, 162 (2014). [Medline](#)
7. V. Bigley, M. Haniffa, S. Doulatov, X. N. Wang, R. Dickinson, N. McGovern, L. Jardine, S. Pagan, I. Dimmick, I. Chua, J. Wallis, J. Lordan, C. Morgan, D. S. Kumararatne, R. Doffinger, M. van der Burg, J. van Dongen, A. Cant, J. E. Dick, S. Hambleton, M. Collin,

- The human syndrome of dendritic cell, monocyte, B and NK lymphoid deficiency. *J. Exp. Med.* **208**, 227–234 (2011). [Medline doi:10.1084/jem.20101459](#)
8. J. L. Casanova, L. Abel, The genetic theory of infectious diseases: A brief history and selected illustrations. *Annu. Rev. Genomics Hum. Genet.* **14**, 215–243 (2013). [Medline doi:10.1146/annurev-genom-091212-153448](#)
 9. J. L. Casanova, M. E. Conley, S. J. Seligman, L. Abel, L. D. Notarangelo, Guidelines for genetic studies in single patients: Lessons from primary immunodeficiencies. *J. Exp. Med.* **211**, 2137–2149 (2014). [Medline doi:10.1084/jem.20140520](#)
 10. K. Honda, H. Yanai, H. Negishi, M. Asagiri, M. Sato, T. Mizutani, N. Shimada, Y. Ohba, A. Takaoka, N. Yoshida, T. Taniguchi, IRF-7 is the master regulator of type-I interferon-dependent immune responses. *Nature* **434**, 772–777 (2005). [Medline doi:10.1038/nature03464](#)
 11. I. Marié, J. E. Durbin, D. E. Levy, Differential viral induction of distinct interferon- α genes by positive feedback through interferon regulatory factor-7. *EMBO J.* **17**, 6660–6669 (1998). [Medline doi:10.1093/emboj/17.22.6660](#)
 12. P. I. Osterlund, T. E. Pietilä, V. Veckman, S. V. Kotenko, I. Julkunen, IFN regulatory factor family members differentially regulate the expression of type III IFN (IFN- λ) genes. *J. Immunol.* **179**, 3434–3442 (2007). [Medline doi:10.4049/jimmunol.179.6.3434](#)
 13. M. Sato, N. Hata, M. Asagiri, T. Nakaya, T. Taniguchi, N. Tanaka, Positive feedback regulation of type I IFN genes by the IFN-inducible transcription factor IRF-7. *FEBS Lett.* **441**, 106–110 (1998). [Medline doi:10.1016/S0014-5793\(98\)01514-2](#)
 14. A. Caillaud, A. G. Hovanessian, D. E. Levy, I. J. Marié, Regulatory serine residues mediate phosphorylation-dependent and phosphorylation-independent activation of interferon regulatory factor 7. *J. Biol. Chem.* **280**, 17671–17677 (2005). [Medline doi:10.1074/jbc.M411389200](#)
 15. R. Lin, Y. Mamane, J. Hiscott, Multiple regulatory domains control IRF-7 activity in response to virus infection. *J. Biol. Chem.* **275**, 34320–34327 (2000). [Medline doi:10.1074/jbc.M002814200](#)

16. I. Marié, E. Smith, A. Prakash, D. E. Levy, Phosphorylation-induced dimerization of interferon regulatory factor 7 unmasks DNA binding and a bipartite transactivation domain. *Mol. Cell. Biol.* **20**, 8803–8814 (2000). [Medline doi:10.1128/MCB.20.23.8803-8814.2000](#)
17. H. Kato, O. Takeuchi, E. Mikamo-Satoh, R. Hirai, T. Kawai, K. Matsushita, A. Hiiragi, T. S. Dermody, T. Fujita, S. Akira, Length-dependent recognition of double-stranded ribonucleic acids by retinoic acid-inducible gene-I and melanoma differentiation-associated gene 5. *J. Exp. Med.* **205**, 1601–1610 (2008). [Medline doi:10.1084/jem.20080091](#)
18. J. Rehwinkel, C. P. Tan, D. Goubau, O. Schulz, A. Pichlmair, K. Bier, N. Robb, F. Vreede, W. Barclay, E. Fodor, C. Reis e Sousa, RIG-I detects viral genomic RNA during negative-strand RNA virus infection. *Cell* **140**, 397–408 (2010). [Medline doi:10.1016/j.cell.2010.01.020](#)
19. H. Kato, O. Takeuchi, S. Sato, M. Yoneyama, M. Yamamoto, K. Matsui, S. Uematsu, A. Jung, T. Kawai, K. J. Ishii, O. Yamaguchi, K. Otsu, T. Tsujimura, C. S. Koh, C. Reis e Sousa, Y. Matsuura, T. Fujita, S. Akira, Differential roles of MDA5 and RIG-I helicases in the recognition of RNA viruses. *Nature* **441**, 101–105 (2006). [Medline doi:10.1038/nature04734](#)
20. M. Yoneyama, M. Kikuchi, T. Natsukawa, N. Shinobu, T. Imaizumi, M. Miyagishi, K. Taira, S. Akira, T. Fujita, The RNA helicase RIG-I has an essential function in double-stranded RNA-induced innate antiviral responses. *Nat. Immunol.* **5**, 730–737 (2004). [Medline doi:10.1038/ni1087](#)
21. P. Staeheli, O. Haller, W. Boll, J. Lindenmann, C. Weissmann, Mx protein: Constitutive expression in 3T3 cells transformed with cloned Mx cDNA confers selective resistance to influenza virus. *Cell* **44**, 147–158 (1986). [Medline doi:10.1016/0092-8674\(86\)90493-9](#)
22. X. Wang, E. R. Hinson, P. Cresswell, The interferon-inducible protein viperin inhibits influenza virus release by perturbing lipid rafts. *Cell Host Microbe* **2**, 96–105 (2007). [Medline doi:10.1016/j.chom.2007.06.009](#)

23. B. Mangeat, L. Cavagliotti, M. Lehmann, G. Gers-Huber, I. Kaur, Y. Thomas, L. Kaiser, V. Piguet, Influenza virus partially counteracts restriction imposed by tetherin/BST-2. *J. Biol. Chem.* **287**, 22015–22029 (2012). [Medline doi:10.1074/jbc.M111.319996](#)
24. M. Dittmann, H. H. Hoffmann, M. A. Scull, R. H. Gilmore, K. L. Bell, M. Ciancanelli, S. J. Wilson, S. Crotta, Y. Yu, B. Flatley, J. W. Xiao, J. L. Casanova, A. Wack, P. D. Bieniasz, C. M. Rice, A serpin shapes the extracellular environment to prevent influenza A virus maturation. *Cell* **160**, 631–643 (2015). [Medline doi:10.1016/j.cell.2015.01.040](#)
25. M. Kerkmann, S. Rothenfusser, V. Hornung, A. Towarowski, M. Wagner, A. Sarris, T. Giese, S. Endres, G. Hartmann, Activation with CpG-A and CpG-B oligonucleotides reveals two distinct regulatory pathways of type I IFN synthesis in human plasmacytoid dendritic cells. *J. Immunol.* **170**, 4465–4474 (2003). [Medline doi:10.4049/jimmunol.170.9.4465](#)
26. A. Izaguirre, B. J. Barnes, S. Amrute, W. S. Yeow, N. Megjugorac, J. Dai, D. Feng, E. Chung, P. M. Pitha, P. Fitzgerald-Bocarsly, Comparative analysis of IRF and IFN- α expression in human plasmacytoid and monocyte-derived dendritic cells. *J. Leukoc. Biol.* **74**, 1125–1138 (2003). [Medline doi:10.1189/jlb.0603255](#)
27. Y. Itoh, K. Shinya, M. Kiso, T. Watanabe, Y. Sakoda, M. Hatta, Y. Muramoto, D. Tamura, Y. Sakai-Tagawa, T. Noda, S. Sakabe, M. Imai, Y. Hatta, S. Watanabe, C. Li, S. Yamada, K. Fujii, S. Murakami, H. Imai, S. Kakugawa, M. Ito, R. Takano, K. Iwatsuki-Horimoto, M. Shimojima, T. Horimoto, H. Goto, K. Takahashi, A. Makino, H. Ishigaki, M. Nakayama, M. Okamatsu, K. Takahashi, D. Warshauer, P. A. Shult, R. Saito, H. Suzuki, Y. Furuta, M. Yamashita, K. Mitamura, K. Nakano, M. Nakamura, R. Brockman-Schneider, H. Mitamura, M. Yamazaki, N. Sugaya, M. Suresh, M. Ozawa, G. Neumann, J. Gern, H. Kida, K. Ogasawara, Y. Kawaoka, In vitro and in vivo characterization of new swine-origin H1N1 influenza viruses. *Nature* **460**, 1021–1025 (2009). [Medline](#)
28. S. X. Huang, M. N. Islam, J. O'Neill, Z. Hu, Y.-G. Yang, Y.-W. Chen, M. Mumau, M. D. Green, G. Vunjak-Novakovic, J. Bhattacharya, H.-W. Snoeck, Efficient generation of lung and airway epithelial cells from human pluripotent stem cells. *Nat. Biotechnol.* **32**, 84–91 (2014). [Medline doi:10.1038/nbt.2754](#)

29. M. E. Conley, J. L. Casanova, Discovery of single-gene inborn errors of immunity by next generation sequencing. *Curr. Opin. Immunol.* **30**, 17–23 (2014). [Medline](#)
[doi:10.1016/j.coi.2014.05.004](https://doi.org/10.1016/j.coi.2014.05.004)
30. J. L. Casanova, L. Abel, L. Quintana-Murci, Immunology taught by human genetics. *Cold Spring Harb. Symp. Quant. Biol.* **78**, 157–172 (2013). [Medline](#)
[doi:10.1101/sqb.2013.78.019968](https://doi.org/10.1101/sqb.2013.78.019968)
31. S. Hambleton, S. Salem, J. Bustamante, V. Bigley, S. Boisson-Dupuis, J. Azevedo, A. Fortin, M. Haniffa, L. Ceron-Gutierrez, C. M. Bacon, G. Menon, C. Trouillet, D. McDonald, P. Carey, F. Ginhoux, L. Alsina, T. J. Zumwalt, X. F. Kong, D. Kumararatne, K. Butler, M. Hubeau, J. Feinberg, S. Al-Muhsen, A. Cant, L. Abel, D. Chaussabel, R. Doffinger, E. Talesnik, A. Grumach, A. Duarte, K. Abarca, D. Moraes-Vasconcelos, D. Burk, A. Berghuis, F. Geissmann, M. Collin, J. L. Casanova, P. Gros, IRF8 mutations and human dendritic-cell immunodeficiency. *N. Engl. J. Med.* **365**, 127–138 (2011). [Medline](#)
[doi:10.1056/NEJMoal100066](https://doi.org/10.1056/NEJMoal100066)
32. M. Pasquet, C. Bellanné-Chantelot, S. Tavitian, N. Prade, B. Beaupain, O. Larochelle, A. Petit, P. Rohrlich, C. Ferrand, E. Van Den Neste, H. A. Poirel, T. Lamy, M. Ouachée-Chardin, V. Mansat-De Mas, J. Corre, C. Récher, G. Plat, F. Bachelerie, J. Donadieu, E. Delabesse, High frequency of GATA2 mutations in patients with mild chronic neutropenia evolving to MonoMac syndrome, myelodysplasia, and acute myeloid leukemia. *Blood* **121**, 822–829 (2013). [Medline](#) [doi:10.1182/blood-2012-08-447367](https://doi.org/10.1182/blood-2012-08-447367)
33. S. Baron, A. Isaacs, Absence of interferon in lungs from fatal cases of influenza. *BMJ* **1**, 18–20 (1962). [Medline](#) [doi:10.1136/bmj.1.5270.18](https://doi.org/10.1136/bmj.1.5270.18)
34. C. Agrati, C. Gioia, E. Lalle, E. Cimini, C. Castilletti, O. Armignacco, F. N. Lauria, F. Ferraro, M. Antonini, G. Ippolito, M. R. Capobianchi, F. Martini, Association of profoundly impaired immune competence in H1N1v-infected patients with a severe or fatal clinical course. *J. Infect. Dis.* **202**, 681–689 (2010). [Medline](#) [doi:10.1086/655469](https://doi.org/10.1086/655469)
35. P. N. Jone, D. D. Ivy, Echocardiography in pediatric pulmonary hypertension. *Front. Pediatr.* **2**, 124 (2014). [doi:10.3389/fped.2014.00124](https://doi.org/10.3389/fped.2014.00124)

36. H. Li, R. Durbin, Fast and accurate short read alignment with Burrows-Wheeler transform. *Bioinformatics* **25**, 1754–1760 (2009). [Medline doi:10.1093/bioinformatics/btp324](#)
37. A. McKenna, M. Hanna, E. Banks, A. Sivachenko, K. Cibulskis, A. Kernysky, K. Garimella, D. Altshuler, S. Gabriel, M. Daly, M. A. DePristo, The Genome Analysis Toolkit: A MapReduce framework for analyzing next-generation DNA sequencing data. *Genome Res.* **20**, 1297–1303 (2010). [Medline doi:10.1101/gr.107524.110](#)
38. H. Li, B. Handsaker, A. Wysoker, T. Fennell, J. Ruan, N. Homer, G. Marth, G. Abecasis, R. Durbin, The Sequence Alignment/Map format and SAMtools. *Bioinformatics* **25**, 2078–2079 (2009). [Medline doi:10.1093/bioinformatics/btp352](#)
39. I. A. Adzhubei, S. Schmidt, L. Peshkin, V. E. Ramensky, A. Gerasimova, P. Bork, A. S. Kondrashov, S. R. Sunyaev, A method and server for predicting damaging missense mutations. *Nat. Methods* **7**, 248–249 (2010). [Medline doi:10.1038/nmeth0410-248](#)
40. M. Kircher, D. M. Witten, P. Jain, B. J. O’Roak, G. M. Cooper, J. Shendure, A general framework for estimating the relative pathogenicity of human genetic variants. *Nat. Genet.* **46**, 310–315 (2014). [Medline doi:10.1038/ng.2892](#)
41. P. C. Ng, S. Henikoff, Predicting deleterious amino acid substitutions. *Genome Res.* **11**, 863–874 (2001). [Medline doi:10.1101/gr.176601](#)
42. S. Purcell, B. Neale, K. Todd-Brown, L. Thomas, M. A. Ferreira, D. Bender, J. Maller, P. Sklar, P. I. de Bakker, M. J. Daly, P. C. Sham, PLINK: A tool set for whole-genome association and population-based linkage analyses. *Am. J. Hum. Genet.* **81**, 559–575 (2007). [Medline doi:10.1086/519795](#)
43. R. McQuillan, A. L. Leutenegger, R. Abdel-Rahman, C. S. Franklin, M. Pericic, L. Barac-Lauc, N. Smolej-Narancic, B. Janicijevic, O. Polasek, A. Tenesa, A. K. Macleod, S. M. Farrington, P. Rudan, C. Hayward, V. Vitart, I. Rudan, S. H. Wild, M. G. Dunlop, A. F. Wright, H. Campbell, J. F. Wilson, Runs of homozygosity in European populations. *Am. J. Hum. Genet.* **83**, 359–372 (2008). [Medline doi:10.1016/j.ajhg.2008.08.007](#)
44. N. Stoletzki, A. Eyre-Walker, Estimation of the neutrality index. *Mol. Biol. Evol.* **28**, 63–70 (2011). [Medline doi:10.1093/molbev/msq249](#)

45. J. S. Yount, T. A. Kraus, C. M. Horvath, T. M. Moran, C. B. López, A novel role for viral-defective interfering particles in enhancing dendritic cell maturation. *J. Immunol.* **177**, 4503–4513 (2006). [Medline doi:10.4049/jimmunol.177.7.4503](#)
46. M. Desforges, J. Charron, S. Bérard, S. Beausoleil, D. F. Stojdl, G. Despars, B. Laverdière, J. C. Bell, P. J. Talbot, C. P. Stanners, L. Poliquin, Different host-cell shutoff strategies related to the matrix protein lead to persistence of vesicular stomatitis virus mutants on fibroblast cells. *Virus Res.* **76**, 87–102 (2001). [Medline doi:10.1016/S0168-1702\(01\)00251-9](#)
47. J. Steel, A. C. Lowen, L. Pena, M. Angel, A. Solórzano, R. Albrecht, D. R. Perez, A. García-Sastre, P. Palese, Live attenuated influenza viruses containing NS1 truncations as vaccine candidates against H5N1 highly pathogenic avian influenza. *J. Virol.* **83**, 1742–1753 (2009). [Medline doi:10.1128/JVI.01920-08](#)
48. X. Yu, T. Tsibane, P. A. McGraw, F. S. House, C. J. Keefer, M. D. Hicar, T. M. Tumpey, C. Pappas, L. A. Perrone, O. Martinez, J. Stevens, I. A. Wilson, P. V. Aguilar, E. L. Altschuler, C. F. Basler, J. E. Crowe Jr., Neutralizing antibodies derived from the B cells of 1918 influenza pandemic survivors. *Nature* **455**, 532–536 (2008). [Medline doi:10.1038/nature07231](#)
49. P. Stafford, Ed., *Methods in Microarray Normalization* (CRC Press, 2008).
50. W. C. Au, W. S. Yeow, P. M. Pitha, Analysis of functional domains of interferon regulatory factor 7 and its association with IRF-3. *Virology* **280**, 273–282 (2001). [Medline doi:10.1006/viro.2000.0782](#)